X-Disciplinarity

DOI: https://doi.org/10.63174/xdi.CVVH6525

Original Article

Longitudinal Manipulation of Optical Lattices Based on Six-Aperture Spiral Array

https://doi.org/10.63174/xdi.CVVH6525

Received: 09 Aug 2025

Accepted: 15 Sep 2025

Published: 17 Sep 2025

Open Access

Shirong Liu[1], Xuanlu Zhang[1] and Li Ma[1*]

Abstract: Optical Lattices are evolving from an information carrier to a programmable medium in which topology, structure and propagation are dynamically coupled. Here we investigated longitudinal manipulation of optical lattices generated by a six-aperture spiral array whose azimuthal phase is imprinted with a topological charge *l*. By varying *l* from 1 to 7 in simulations, we sculpted the longitudinal lattices into Hexagonal, Kagome, and Honeycomb structures, whose transverse phase profiles are uniquely encoded by topological phase configurations. The results demonstrated that the phase profiles execute a longitudinal pulsation, while all higher-order vortices converge to a stable zero state after a geometry-dependent length *z*. During the longitudinal variations, the measured phase-lattice exhibits the correspondences of 6π-Honeycomb, ±4π-Kagome, and ±2π-Hexagon, enabling predictive design of reconfigurable photonic crystals and topologically protected registers. Our results establish the six-aperture spiral as a compact diffractive engine for coherent lattice reconfiguration and open a route to longitudinal light-matter interfaces.

1. Introduction

Optical lattices, as a significant form of structured light fields, have attracted extensive attention due to their spatial periodicity and tunability, showing broad application prospects in optical manipulation [1,2,3], quantum simulation [4], precision measurement [5], and information encoding [6,7]. Generated through the interference of multiple coherent laser beams, optical lattices establish periodic optical potentials that enable exquisite control over microscopic particles and quantum systems. Within such lattice architectures, optical vortices emerge as fundamental building blocks for constructing complex spatial configurations. Characterized by their helical wavefronts and quantized topological charges [8,9], these vortex beams possess intrinsic orbital angular momentum, a property first systematically articulated by Allen et al. [10] that underpins their distinctive phase evolution during propagation. The topological charge, in particular, exerts a profound influence on determining both the spatial structure and propagation dynamics of the resultant light field [11], thereby affording longitudinal-manipulation degrees of freedom for advancing optical lattice-based technologies. Recent studies on multi-spiral structures have further highlighted the potential of tailored aperture arrays in regulating vortex dynamics [12,13].

In recent years, significant advancements have been made in the study of two-dimensional (2D) planar structures of optical lattices. For example, photonic quasicrystals, constructed through multi-beam interference, have unveiled the ring-like distribution of vortices within lattices [14]. Additionally, 2D photonic crystal slabs have achieved notable success in manipulating light-field parameters in momentum space [15]. However, in contrast to planar characteristics, the longitudinal properties of optical lattices remain relatively underexplored. In practical applications such as long-distance optical communication, multilayer optical data storage, and quantum information transmission, the longitudinal evolution of optical lattices directly impacts system stability and performance [14,16]. Currently, systematic studies on the mechanisms of phase evolution, topological stability, and the coupling relationships between propagation distance and lattice structures are still insufficient, which limits further applications in related fields, particularly in the context of emerging spiral-array-based manipulation strategies [17,18].

Building upon the significance of longitudinal manipulation of optical lattices and vortices, it is crucial to address the limitations of conventional generation methods. Traditional approaches for creating optical lattices, such as those relying on fixed laser interference patterns [15], often suffer from constrained tunability and fixed structural configurations [19,20]. For instance, in the context of generating optical lattices for specific applications like optical trapping in micro-manipulation, the fixed-structure nature of traditional methods restricts the adaptability to different particle sizes and types [1,21]. This poses significant challenges to the flexible manipulation of lattice architectures. In contrast, multi-aperture interference methods have emerged as a promising alternative to circumvent these limitations, offering enhanced controllability over lattice formation and vortex dynamics [22,23]. Among such approaches, six-aperture interference configurations exhibit distinct advantages in lattice research: they enable precise regulation of interference patterns through aperture arrangement, facilitating the generation of complex lattice structures with tailored topological properties. The orbital angular momentum associated with optical vortices in these configurations, as first systematically studied by Allen et al. [10,24], plays a key role in determining the lattice characteristics. While existing studies have extensively explored the transverse characteristics of six-aperture interference systems, research leveraging this interference principle to investigate longitudinal behaviors remains relatively sparse, leaving a critical gap in understanding the full spatiotemporal dynamics of optical lattices.

This paper systematically investigates the longitudinal manipulation of optical lattices utilizing a six-aperture spiral array structure. The six-aperture spiral array employed in this study features a specific geometric arrangement: six apertures are distributed uniformly along a spiral trajectory with adjustable parameters, including spiral pitch, initial radius, and angular spacing between adjacent apertures. By establishing a plane-wave propagation model in conjunction with numerical simulations, we analyze the intensity distribution, phase evolution, and variations in the topological structure of lattices with different topological charges during propagation. The theoretical basis for understanding phase evolution and phenomena related to topological charge is established through our analysis of how the propagation of optical vortices depends on their topological charge. Furthermore, we elucidate the synergistic mechanism between propagation distance and topological charge.

2. Research Methods and Physical Models

2.1. Structure of the Spiral Six-aperture Screen

We present a spiral multi-aperture diffraction system for longitudinal light-field manipulation, as shown in **Figure 1**(a). Figure 1(a) depicts the spiral six-aper-

[1] Department of Physics, Changzhi University, Changzhi 046011, China
[*] Corresponding Author: mali9001@126.com

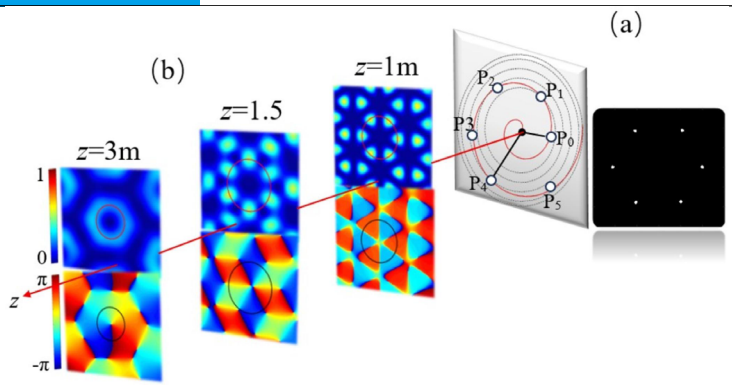

Figure 1. **Spiral six-aperture screen schematic and diffraction patterns.** (a) Schematic model of the spiral six-aperture screen; (b) Intensity and phase patterns at characteristic diffraction distances for topological charge l=3.

ture screen, where six apertures with labeles from P_0 to P_5 are distributed in a rotationally symmetric manner. P_0 is situated close to the center, while P_1 to P_5 are arranged along a spiral path that emits outward from P_0. Each adjacent pair among P_0 to P_5 is separated by an azimuthal angle of $\pi/3$, which gives the entire aperture array a sixfold rotational symmetry. This spiral arrangement, with P_0 as the reference at the initial radial position, realizes a layout that with a radial gradient characteristic. Six apertures are arranged along a spiral defined by the equation $r=r_0+\kappa\theta$, where r is the radial distance from a point to the origin in polar coordinates, r_0 is the initial radial distance of the spiral with θ=0, κ is the expansion rate of the spiral and describes how the spiral expands with changes in angle, and θ is the azimuthal angle in polar coordinates. These apertures are positioned with an azimuthal increment of $\pi/3$, forming a sixfold rotationally symmetric structure. This structure integrates central symmetry and radial gradient, enabling simultaneous azimuthal phase encoding and radial optical path encoding [23]. The diffraction model reveals that progressive increases in optical path length from individual apertures introduce wavelength-dependent phase shifts via optical path differences relative to the central aperture. Six-beam interference via complex-amplitude summation generates a helical phase-modulated lattice, where periodic phase differences from fixed angular increments and radial optical path difference gradients jointly enable dynamic tuning of fringe structure and spatial frequency. Optical properties are tailored by spiral parameters. The expansion rate (κ) dictates the dimensions of the central primitive cell, with an increased κ diminishing the central optical path difference to yield broader interference striations. The radial gradient governs transitions in striation density, with steeper gradients augmenting the spatial frequency in peripheral regions. Aperture-specific amplitude modulation further facilitates longitudinal phase control and intensity gradation within the plane, thereby elevating the precision of light-field engineering.

2.2. Typical Structure Optical Lattices

In simulations, plane wave illuminates a spiral six-aperture as shown in Figure 1(a). For the configuration with topological charge or topological state l=3, we investigate lattice formations and vortex characteristics on the observation plane. Simulated intensity patterns and phase distributions as shown in Figure 1 (b) reveal distinct optical lattices at varying diffraction distances (z). When the aperture is at a normalized distance z=1m, with a spiral opening parameter inducing a 6π phase shift per cycle, a Honeycomb lattice forms, which exhibits a cluster-like intensity pattern with a regular six-petal morphology. At z=1.5m, with the same aperture and the spiral opening parameter producing a -4π phase shift per cycle, a Kagome lattice featuring a central second-order vortex emerges. Its phase distribution exhibits a double 2π cycles around the phase singularity, characterized by two discontinuous jumps from +π to -π, with stellate intensity spots forming the lattice structure. At z=3m with a -2π phase shift per cycle, a Hexagonal lattice forms containing a central first-order vortex, where the phase varies uniformly through a single 2π cycle around the singularity and the intensity displays regular Hexagonal symmetry.

Analysis of these fundamental lattice units via the phase vortex framework identifies characteristic configurations: a Hexagonal lattice in optics refers to a two-dimensional arrangement of light fields where each site is surrounded by six nearest neighbors, forming a regular hexagon pattern; a Honeycomb lattice is composed of two interpenetrating triangular sublattices arranged in a hexagonal pattern, where each site has three nearest neighbors instead of six, leading to distinct physical properties; a Kagome lattice consists of corner-sharing triangles arranged in a hexagonal tiling, with each site connected to four neighbors, giving rise to a mixture of hexagonal and triangular motifs. These simulations confirm that a six-aperture with spiral-distributed openings generates diverse cluster lattice morphologies and vortex arrays carrying distinct orbital angular momenta, validating the structural characteristics of these lattices.

3. Numerical Simulations

3.1. Numerical Simulation of Optical Lattices

In the numerical simulation of optical lattices, we employ the angular spectrum propagation method to investigate the longitudinal manipulation characteristics of vortex arrays in free space. The implementation procedure is structured as follows: First, the computational domain is initialized by defining the side length and sampling points to satisfy the sampling theorem, after which the complex amplitude distribution of the initial vortex field with a specified topological charge is constructed. Subsequently, spatial confinement is introduced via an aperture function, while amplitude modulation is applied using a radial modulation function to emulate the effects of optical apertures and beam shaping in practical systems. The propagation dynamics are governed by a transfer function derived from Fresnel diffraction theory, which encodes the phase delay in the spatial frequency domain and captures the wavefront evolution during diffraction. By leveraging fast Fourier transforms, the modulated initial field is convolved with the propagation kernel in the spectral domain, and an inverse transform yields the propagated field distribution. This framework rigorously adheres to scalar diffraction theory, enabling precise characterization of the dynamic evolution of vortex phase singularities. As such, it serves as a versatile numerical tool for analyzing structured light propagation in optical lattices, particularly in advanced studies involving coupled multi-vortex arrays and topological charge manipulation.

3.2. Intensity Evolutions of Optical Lattices

Figure 2 presents a series of simulation images demonstrating the evolution of intensity distributions in optical lattice across topological charges l=1-7 during propagation. Images are grouped by charge: l=1-2 (Group 1), l=3-4 (Group 2), and l=5-7 (Group 3). The topological charge, which governs the azimuthal phase gradient, is a fundamental parameter defining the properties of optical lattice, and the simulations systematically cover the evolution characteristics of optical lattices during propagation within this parameter range.

For the l=1 lattice, the red circle denotes the primitive cell, and intensity distributions were analyzed at propagation distances z=0.5m, 0.75m, 1m, 1.5m, and 2.5m. At z=0.5m, the primitive cell exhibits bright spots organized into a Kagome-characteristic triangular network, where adjacent spots form interlocking triangles. This distribution builds up the Kagome lattice. At z=1m, within the Hexagonal lattice framework, the primitive cell exhibits an annular intensity profile. It features a bright, closed-periphery ring with a central null, characteristic of the Hexagonal lattice's structural signature at this propagation distance. This annular profile, characteristic of first-order vortices, further constitutes the Hexagonal vortex lattice within the framework. As z increases, field evolution occurs within the Hexagonal framework. At z=2.5, the first-order vortex signatures vanish, and the structure evolves into a symmetric lattice of bright, compact cores. Each core shows concentric intensity decay, forming a pattern with distinct, regularly-spaced bright spots that departs from the annular vortex profile. For the l=2 lattice, we investigated the variations of the optical lattice at different propagation distances. At z=0.5m, the structure remains a Kagome lattice. It evolves into a symmetric, six-petal-like Honeycomb lattice

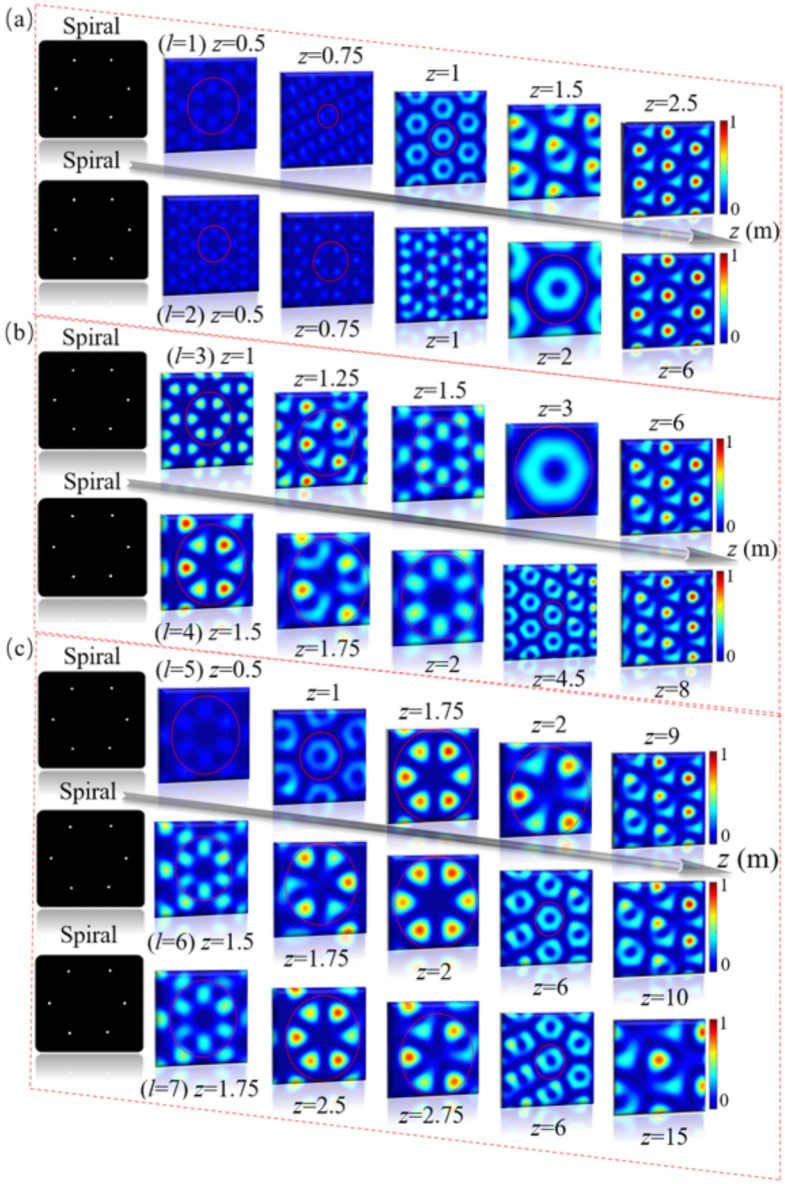

Figure 2. Lattices generated by a six-aperture spiral array and central intensity patterns for each order. (a) *l*=1 and 2; (b) *l*=3 and 4; (c) *l*=5, 6 and 7.

by *z*=0.75m, reverts to a brighter Kagome lattice at *z*=1m, transforms into a Hexagonal lattice at *z*=2m, and finally forms concentric rings with maximum intensity at the center and gradual outward decay by *z*=6m. For the *l*=3 lattice, structural transitions were observed across propagation distances. At *z*=1m, it presents a Honeycomb lattice. By *z*=1.25m, the intensity pattern evolves into a three-lobed form, further transitioning to a Kagome lattice at *z*=1.5m. It transforms into a Hexagonal lattice at *z*=3m and finally reverts to the same concentric ring pattern with central maximum intensity and outward decay by *z*=6m. For the *l*=4 lattice, morphological variations occur with increasing *z*. At initial propagation stages, it exhibits a distinct lattice configuration, evolving through characteristic structural transitions before transforming into a Hexagonal lattice at an intermediate distance (e.g., *z*=4m) ultimately converging to the identical concentric ring pattern by *z*=6m.

In summary, the lattices corresponding to *l*=5, 6, and 7 exhibit analogous evolutionary behaviors. As optical lattices with topological charges *l*=1-7 propagate, they traverse Hexagonal, Kagome, and Honeycomb lattices, with their intensity distributions evolving dynamically alongside the propagation distance.

3.3. Phase Evolutions of Optical Lattices

The simulation analysis of phase evolution in optical lattices (topological charges *l*=1-7) as a function of propagation distance reveals characteristic distributions. First, multi-order commonalities exhibit volatility. As illustrated in **Figure 3**, the seven curves corresponding to *l*=1-7 demonstrate that the central phase evolves non-monotonically with propagation distance. During the initial propagation stage, rapid phase oscillations are observed. While fluctuations persist with increasing *z*, the phase eventually stabilizes at zero, reflecting the fundamental phase dynamics in optical lattice propagation. Second, order-dependent behavior is evident, with enhanced initial pulsation observed at higher azimuthal indices. A comparative analysis across Figure 3(a)-3(c) indicates that the *l*=1 field exhibits moderate initial fluctuations (approximately ±4π), whereas higher-order vortices (*l*=3, 5, 7) display significantly amplified oscillations. The *l*=3 trajectory (purple) reaches -6π in the near-field region, while the *l*=5 (pink) and *l*=7 (cyan) trajectories exhibit larger initial amplitudes and complex oscillatory pathways. This heightened initial volatility reflects increased wavefront complexity associated with higher topological charges. Finally, phase distributions converge toward zero stability at sufficient propagation distances. Regardless of *l*, when *z* exceeds order-dependent thresholds (*z*>2m for *l*=1; *z*>6m for *l*=5; *z*>10m for *l*=7), fluctuation amplitudes narrow substantially and stabilize to zero. This establishes that optical lattice core phases attain steady states after sufficient propagation, with higher orders requiring longer stabilization distances.

In summary, vortex core phase distributions exhibit strong dependence on topological charge, featuring initial oscillations and eventual stabilization at zero phase. Higher-order fields manifest intensified initial phase volatility, revealing

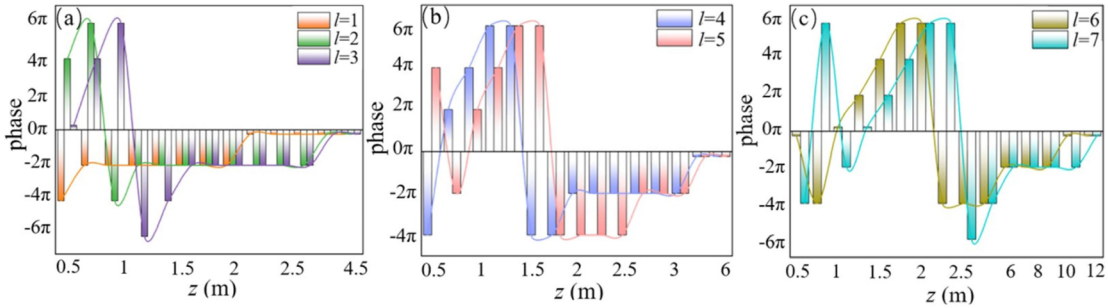

Figure 3. Phase evolutions with distance for each order. (a) *l*=1-3; (b) *l*=4-5; (c) *l*=6-7. Bar charts show phase values, and colored lines represent fitted curves.

fundamental implications for optical lattice phase evolution dynamics.

4. Results and Discussion

4.1. Regular Structure of Optical Lattices

During the propagation of optical lattices, a distinct correlation exists in specific regions between phase states and optical lattice configurations, forming the fundamental basis for structured light manipulation. Analysis of **Figure 4** reveals consistent phase-intensity relationships across topological charges. When phase is precisely controlled at 6π, the field achieves uniformity and stabilizes into Honeycomb lattices. This 6π condition acts as a critical transitional state prior to the final formation of lattices: simulations confirm that Hexagonal primitive cells arrange regularly with characteristic topological order, offering precise phase targets for the directed generation of Honeycomb lattices. At ±4π phases, fields uniformly evolve into Kagome lattices. Vortex fields across orders exhibit petal-like lobes with intensity nulls within primitive cells at these phase points, confirming phase-specific Kagome formation and enabling on-demand lattice construction. Similarly, ±2π phases yield stable Hexagonal lattices, where specific configurations exhibit distinctive features: central phase singularities surrounded by annular intensity profiles. Such consistency provides a basis for controlled Hexagonal lattice generation.

4.2. Invariance of Phase-Lattice Correspondence

Optical lattices exhibit distinct phase-structure correspondences during longitudinal evolution, specifically 6π-Honeycomb, ±4π-Kagome, and ±2π-Hexagonal. To validate the regularity, a cross-comparative analysis of simulation data for *l*=1, 4, and 6 lattices was performed, revealing strong morphological consistency at identical phase values. As evidenced in Figure 4, distinct topological charges show exhibit identical optical lattice morphologies. Representative cases include the *l*=1 field forming a Hexagonal lattice at *z*=1.25m under a -2π phase (Figure 4a), the *l*=4 field maintaining Hexagonal ordering at *z*=4m under

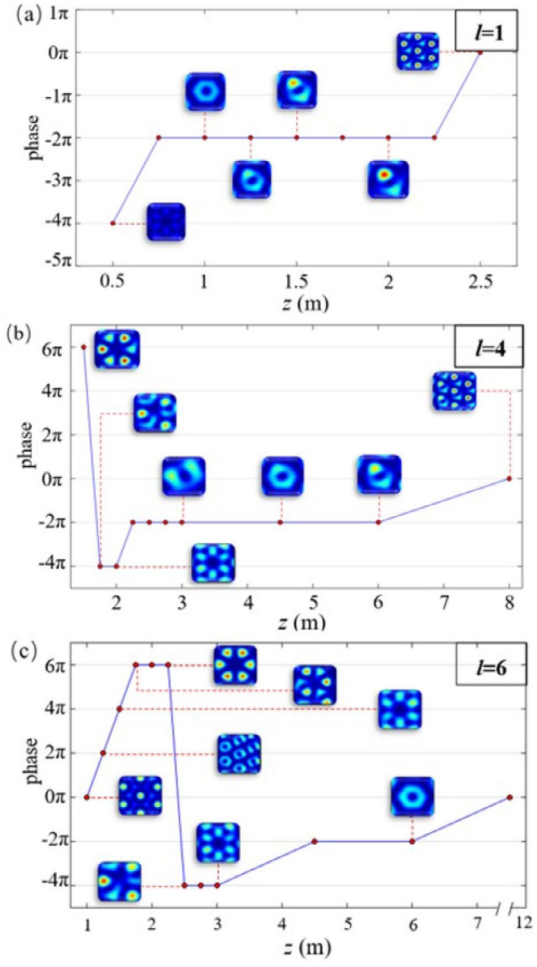

Figure 4. Intensity-phase correlation diagrams of optical lattices for different orders. (a) *l*=1; (b) *l*=4; (c) *l*=6. The blue polyline shows the phase-distance variation trend.

a -π phase (Figure 4b), and the *l*=6 field displaying a stable Hexagonal configuration at *z*=6m under a -2π phase (Figure 4c). In these cases, it is confirmed that the 6π-Honeycomb, ±4π-Kagome, and ±2π-Hexagonal correspondences hold across topological charges. This invariance underpins the predictive manipulation of lattice configurations and enables the design of reconfigurable photonic crystals and topologically protected registers.

5. Conclusion

This study focuses on the longitudinal manipulation mechanism of optical lattices based on a six-aperture spiral array. It adopts a research method combining computational modeling and numerical simulation to conduct systematic research and takes three typical optical lattices, Hexagonal, Kagome and Honeycomb lattices, as research objects and conducts in-depth analysis of their intrinsic characteristics through computational modeling. It establishes correlations between the longitudinal manipulation behavior of optical lattices and the structural parameters of the six-aperture spiral array. The study then performs systematic numerical simulations in optical lattices with topological charges *l*=1-7, focuses on exploring their evolutionary regularities during longitudinal propagation, and finally reveals two key longitudinal propagation phenomena. The first is that the optical lattice phases exhibit oscillations varying with propagation distance (*z*) during longitudinal propagation, with higher topological charges leading to stronger initial fluctuations and eventual stabilization at zero phase. The second is that during longitudinal evolution, the optical lattice exhibits phase-structure correspondences of 6π-Honeycomb, ±4π-Kagome, and ±2π-Hexagonal, which underpins the predictive manipulation of lattice configurations. This research advances practical understanding of longitudinal manipulation of optical lattices and provides key foundational support for applications in photonic crystal engineering, controlled light field propagation, and related fields.

Conflict of Interest

The author Li Ma is an editor of *X-Disciplinarity*, but was not involved in the peer review or decision-making process for this article.

Author Contributions

Shirong Liu did Writing–original draft, Data curation, Formal analysis, Software, Visualization. Xuanlu Zhang did Data analysis, Visualization. Li Ma did Writing–review & editing, Methodology, Conceptualization, Supervision.

Acknowledgements

This work was supported by Applied Basic Research Project of Shanxi Province (No. 202403021212017), and Scientific and Technological Innovation Programs of Higher Education Institutions in Shanxi (STIP) (No. 2024L349).

References

[1] A. Ashkin. “Acceleration and trapping of particles by radiation pressure.” *Phys. Rev. Lett.* **1970**, *24*, 4-26, 156-159.
[2] S. Tao, X-C. Yuan, J. Lin, X. Peng, H. Niu. “Fractional optical vortex beam induced rotation of particles.” *Opt. Express*, **2005**, *13*, 20, 7726-7731.
[3] W. M. Lee, X. - C. Yuan, W. C. Cheong. “Optical vortex beam shaping by use of highly efficient irregular spiral phase plates for optical micromanipulation.” *Opt. Lett.*, **2004**, *29*, 15, 1796-1798.
[4] J. M. Hickmann, E. J. S. Fonseca, W. C. Soares, S. Chávez-Cerda. “Unveiling a truncated optical lattice associated with a triangular aperture using light’s orbital angular momentum.” *Phys. Rev. Lett.* **2010**, *105*, 5, 053904.
[5] Z. Shen, Z. J. Hu, G. H. Yuan, C. J. Min, H. Fang, X. - C. Yuan. “Visualizing orbital angular momentum of plasmonic vortices.” *Opt. Lett.* **2012**, *37*, 22, 4627-4629.
[6] A. Vaziri, J. -W. Pan, T. Jennewein, G. Weihs, A. Zeilinger. “Concentration of higher dimensional entanglement: qutrits of photon orbital angular momentum.” *Phys. Rev. Lett.*, **2003**, *91*, 22, 227902.
[7] Z. W. Xie, T. Lei, F. Li, H. D. Qiu, Z. C. Zhang, H. Wang, C. J. Min, L. P. Du, Z. H. Li, X. C. Yuan. “Ultra-broadband on-chip twisted light emitter for optical communications.” *Light Sci. Appl.* **2018**, *7*, 4, 18001.
[8] N. R. Heckenberg, R. McDuff, C. P. Smith, A. G. White, H. Rubinsztein - Dunlop. “Generation of optical phase singularities by computer - generated holograms.” *Opt. Lett.* **1992**, *17*, 3, 221-223.
[9] M. Uchida, A. Tonomura. “Generation of electron beams carrying orbital angular momentum.” *Nature*, **2010**, *464*, 7289, 737-739.
[10] L. Allen, M. J. Padgett, M. Babiker. “The orbital angular momentum of light.” *Prog. Opt.* **1999**, *39*, 291-372.
[11] P. Vaity, R. P. Singh. “Topological charge dependent propagation of optical vortices under quadratic phase transformation.” *Opt. Lett.*, **2012**, *37*, 8, 1301-1303.
[12] L. Ma, C. Chen, Z. Zhan, Q. Dong, C. Cheng, C. Liu. “Generation of spatiotemporal optical vortices in ultrashort laser pulses using rotationally interleaved multispirals.” *Opt. Express*, **2022**, *30*, 26, 47287-47303.
[13] J. Wang, X. Yang, P. Li, L. Ma. “Longitudinal evolution of phase vortices generated by rotationally interleaved multi-spiral.” *Opt. Express*, **2024**, *32*, 9, 15433-15443.
[14] D. J. Richardson, J. M. Fini, L. E. Nelson. “Space-division multiplexing in optical fibres.” *Nat. Photonics*, **2013**, *7*, 5, 354-362.
[15] J. C. T. Lee, S. J. Alexander, S. D. Kevan, S. Roy, B. J. McMorran. “Laguerre–Gauss and Hermite–Gauss soft X-ray states generated using diffractive optics.” *Nat. Photonics.* **2019**, *13*, 3, 205-209.
[16] L. P. Gong, B. Gu, G. H. Rui, Y. P. Cui, Z. Q. Zhu, Q. W. Zhan. “Optical forces of focused femtosecond laser pulses on nonlinear optical Rayleigh particles.” *Photonics Res.* **2018**, *6*, 2, 138-143.
[17] M. Li, Y. Wang, Y. Zhang, M. X. Hua, G. Z. Miao, H. Y. Yijun, L. Ma. “Topological optical field manipulation via double-spiral multi-pinhole arrays.” *X-Disciplinarity* **2025**, *1*, 1, 6.
[18] N. C. Zambon, P. St-Jean, M. Milićević, A. Lemaître, A. Harouri, L. Le Gratiet, O. Bleu, D. D. Solnyshkov, G. Malpuech, I. Sagnes, S. Ravets, A. Amo, J. Bloch. “Optically controlling the emission chirality of microlasers.” *Nat. Photonics.* **2019**, *13*, 4, 283-288.
[19] M. Padgett, R. Bowman. “Tweezers with a twist.” *Nat. Photonics*, **2011**, *5*, 6, 343-348.
[20] S. C. Chapin, V. Germain, E. R. Dufresne. “Automated trapping, assembly, and sorting with holographic optical tweezers.” *Opt. Express*, **2007**, *14*, 26, 13095-13100.
[21] Y. Q. Zhang, J. F. Shen, C. J. Min, Y. F. Jin, Y. Q. Jiang, J. Liu, S. W. Zhu, Y. L. Sheng, A. V. Zayats, X. C. Yuan. “Nonlinearity-induced multiplexed optical trapping and manipulation with femtosecond vector beams.” *Nano Lett.* **2018**, *18*, 9, 5538-5543.
[22] V. V. Kotlyar, A. A. Almazov, S. N. Khonina, V. A. Soifer, H. Elfstrom, J. Turunen. “Generation of phase singularity through diffracting a plane or Gaussian beam by a spiral phase plate.” *J. Opt. Soc. Am. A* **2005**, *22*, 5, 849-861.
[23] A. Bekshaev, O. Orlinska, M. Vasnetsov. “Optical vortex generation with a ‘fork’ hologram under conditions of high-angle diffraction.” *Opt. Commun.*, **2010**, *283*, 10, 2006-2016.
[24] N. Yu, P. Genevet, M. A. Kats, F. Aieta, J. - P. Tetienne, F. Capasso, Z. Gaburro. “Light Propagation with Phase Discontinuities: Generalized Laws of Reflection and Refraction.” *Science* **2011**, *334*, 6054, 333-337.